International Journal of Dairy Technology

SDT Society of Dairy Technology

doi: 10.1111/1471-0307.12797

ORIGINAL RESEARCH

Pilot-scale production and physicochemical characterisation of spray-dried nanoparticulated whey protein powders

JACOB R GURALNICK,[1] RAM R PANTHI,[1] FRANCESCA BOT,[1] VALERIA L CENINI,[2] BARRY MG O'HAGAN,[2] SHANE V CROWLEY[1] and JAMES A O'MAHONY[1]*

[1]*School of Food and Nutritional Sciences, University College Cork, Cork, Ireland, and* [2]*Bioimaging Core Facility Unit, Biomedical Science Research Institute, Ulster University, Coleraine, Northern Ireland, UK*

Spray-dried whey protein isolate (WPI) powders were prepared at pilot-scale from solutions without heat (WPI_{UH}), heated (WPI_H) or heated with calcium (WPI_{HCa}), which were analysed and compared with a control sample (WPI_C). WPI_C, WPI_{UH}, WPI_H and WPI_{HCa} solutions had whey protein denaturation levels of 0.0, 3.2, 64.4 and 74.4%, respectively. Computerised tomography scanning showed that 52.6, 84.0, 74.5 and 41.9% of WPI_C, WPI_{UH}, WPI_H and WPI_{HCa} powder particles had diameters of ≤30 μm. WPI_{HCa} and WPI_H powders were cohesive, while WPI_C and WPI_{UH} powders were easy flowing. Marked differences in microstructure were observed between WPI_H and WPI_{HCa}. There were no measured differences in wall friction, bulk density or colour.

Keywords Whey protein, Nanoparticles, Aggregation, Powder, Physical properties.

INTRODUCTION

In the food industry, demand for high-protein dairy powders, such as whey protein isolate (WPI), has been increasing over the last decade (Lagrange *et al*. 2015). This is because these powders provide a high-quality protein source and have a wide range of functional properties desired during processing and in finished product applications. However, multiple factors, including instability to heat and pH, low bulk density, poor wettability and powder solubility, have limited the applications of these ingredients. Uncontrolled denaturation and aggregation of whey proteins during thermal processing influence powder microstructure, which negatively impacts powder solubility and bulk handling properties (Nuzzo *et al*. 2017; Both *et al*. 2018). Controlling the size of aggregates by thermal processing is a key strategy to address heat-induced instability of whey proteins (Çakir-Fuller 2015), with production of aggregated whey protein structures allowing for tailored properties that may improve heat stability and/or the rehydration properties of resultant powders.

Whey proteins, like most globular proteins, rely on a combination of hydrophobic, covalent and hydrogen bonds to maintain their three-dimensional structures. Additionally, the functional properties of whey protein ingredients are often altered by modifying β-lactoglobulin (β-lg), which is highly heat-labile and a major constituent of whey protein (Foegeding *et al*. 2002). Heat- and mineral-induced aggregation of β-lg allows for disulphide bonding and electrostatic shielding/salt bridges to form within and between whey protein molecules. Consequent changes to the structure of whey proteins alter the behaviour of such protein ingredients during processing and in finished products (Bouaouina *et al*. 2006; Sinha *et al*. 2007) as well as changes to the physical properties of resultant powders (Hogan and O'Callaghan 2013). Notably, whey proteins can form different structures (e.g. strands, fibrils) depending on the exact thermal processing parameters employed (Akkermans *et al*. 2008).

Previous work has demonstrated that microstructural properties of WPI powders can influence their physicochemical and functional

*Author for correspondence. E-mail: sa.omahony@ucc.ie

properties (Barone *et al*. 2019). Generally, a high proportion of native whey proteins on the exterior of whey protein concentrate (WPC) and WPI powders results in smooth powder particle surfaces, while higher proportions of denatured whey proteins result in microwrinkles on the surfaces of such powders (Both *et al*. 2018). Furthermore, denaturation and aggregation of whey proteins increase the hydrophobicity of powder surfaces (Gaiani *et al*. 2010). Therefore, understanding how powder microstructure is affected by denaturation and aggregation of whey proteins will help with controlling and predicting the physical and flow properties thereof.

The poor wetting performance of WPI powders is greatly influenced by physical properties, such as occluded air, particle size and density. Furthermore, WPI typically is dried at a lower total solid content (~20%) compared with more traditional dairy ingredients like skim and whole milk powder (~50%), which in turn influences the powder density, particle size and levels of occluded air. The traditional methodology used to measure occluded and interstitial air uses density (bulk, tapped and particle) through gas displacement measurements (Schuck *et al*. 2007). Computerised tomography (CT) generates high-quality images by applying X-rays to measure air voids, which are then differentiated into occluded and interstitial air; this differentiation could further our understanding of the impact of microstructure on occluded air content of next-generation dairy protein powders. Additional physical properties, such as density, particle size and microstructure, influence flowability, a key quality attribute of powders (Kim *et al*. 2005a).

Previous studies have focused on how increasing the outlet temperature of spray-drying increases whey protein denaturation in resultant powders (Anandharamakrishnan *et al*. 2007), the stability of whey protein aggregates produced from WPI and β-lg in salt solutions (Ryan *et al*. 2012) and characteristics of whey protein aggregates made from WPC solutions (Meza *et al*. 2019). Furthermore, other studies have examined the effects of temperature and the addition of calcium on the formation of whey protein aggregates (Ooi 2015; Buggy *et al*. 2018) and the implications of differences therein for viscosity and colloidal stability of nutritional beverages (e.g. infant formula) (Joyce *et al*. 2017). However, no information is available in the published literature on the effects of controlled denaturation and aggregation on the physicochemical properties of WPI powders.

The overall objective of this study was to determine the influence of heat- and mineral-induced denaturation and aggregation of whey proteins on the physicochemical properties of WPI powders. The physical properties (e.g. particle size, flowability, bulk density) of WPI powders prepared from whey protein solutions treated at 90 °C, with or without 2.5 mM added calcium chloride (i.e. with or without colloidally stable nanoparticulated whey protein aggregates), were assessed to determine how controlling whey protein aggregate size would impact the physicochemical properties of resultant powders. This new knowledge will underpin the targeted modification of physical properties of WPI powders to better suit selected applications.

MATERIALS AND METHODS

Materials

Whey protein isolate (WPI; BiPro®), with 94.4 ± 1.61% protein, was provided by Agropur (Granby, Quebec, Canada). Calcium chloride (1 M) and all other chemicals and reagents were obtained from Sigma-Aldrich (St. Louis, MO, USA).

Preparation of whey protein solutions

Whey protein isolate powder was dissolved in stock calcium chloride solutions with calcium concentration in the range 0.0–4.5 mM (increasing in 0.5 mM increments) in ultrapure water at 8 and 10% protein (w/v). After the pH was measured and adjusted to pH 7.00 (±0.01), the dispersions were allowed to rehydrate fully for 18 h at 4 °C. The solutions were then prepared to volume and pH re-adjusted to 7.00 (±0.01), as required.

Thermal processing of whey protein solutions

Whey protein isolate solutions with different calcium concentrations were heated using a controlled-stress rheometer (AR-G2, TA Instruments, New Castle, DE, USA) equipped with a starch pasting cell; samples were conditioned at 20 °C and with a constant shear of 15 s^{-1} throughout, heated using a ramp of 10 °C/min until the peak temperature (80, 85 or 90 °C) was achieved and held for 30, 60, 90 or 120 s, after which samples were cooled at 10 °C/min to 20 °C following the method of Joyce *et al*. (2017).

Whey protein denaturation

Whey protein denaturation was measured using high-performance liquid chromatography based on a variant of the methodology of Huppertz *et al*. (2004), as described in detail by Joyce *et al*. (2017).

Whey protein particle size

The effects of heat- and mineral-induced aggregation on the particle size distribution of whey protein solutions were determined by dynamic light scattering using a Zetasizer Nano ZS (Malvern Instruments, Malvern, UK) particle size analyser, equipped with Malvern Zetasizer software 7.02. Samples were diluted 1:200 in ultrapure water, measured at 25 °C, using a viscosity parameter of 0.8872 cP, refractive index of 1.45 and absorbance of 0.001.

Spray-drying of whey protein solutions

Whey protein solutions required for pilot-scale production of corresponding powders were prepared as described in

preparation of whey protein solutions, with some modifications based on the results from preliminary trials. The thermal treatment chosen to achieve extensive controlled nanoparticulation of whey proteins prior to spray-drying was 10% protein, 2.5 mM calcium, 90 °C peak temperature and 30 s hold time (WPI_{HCa}). A heated control powder (WPI_H) was prepared using conditions of 0.0 mM calcium, 90 °C peak temperature and 30 s hold time, while an unheated control sample (WPI_{UH}) was also prepared. Thermal processing was applied to WPI solutions using a high-temperature short-time Microthermics instrument (Microthermics, Raleigh, NC, USA), at a batch size of 60 L using a constant flow rate of 1 L/min. All three whey protein solutions (i.e. WPI_{UH}, WPI_H and WPI_{HCa}) were then spray-dried using a Niro 25 single-stage spray-dryer (GEA, Søborg, Denmark) with inlet and outlet temperatures of 180 °C and 80 °C, respectively. The total solid content of the feed material was ~10.6%, and evaporation was not used in the production to prevent any further heat-induced aggregation. The original WPI powder was included in subsequent analysis as a reference sample (WPI_C).

Compositional analysis

Protein and moisture were determined using the Kjeldahl nitrogen analysis method with a nitrogen to protein conversion factor of 6.38 (IDF 2014) and oven-drying at 103 °C (IDF 2004), respectively. Fat content was determined by hydrolysing powders in 4 M HCl, with fat extracted from the filtrates through an ST 255 Soxtec 230 V (Foss Analytics, Hillerød, Denmark) with a 5:2 petroleum ether:absolute alcohol mixture. Ash was determined by dry-ashing using a muffle furnace at 800 °C for 8 h (Gaucheron 2010), and carbohydrate was determined by difference.

Colour

Colour of WPI powders was measured using a CR-400 colorimeter (Konica Minolta, Tokyo, Japan) with data for L^* (0 = black, 100 = white), a^* (positive = red, negative = green) and b^* (positive = yellow, negative = blue) colour chromaticity coordinates reported. The powder was analysed in a custom-designed cell, and photographs were taken as described by Amagliani *et al*. (2016). ΔE was calculated using the Commission on illumination (CIE) 2000 equation.

Powder microstructure

All microstructural analyses of the WPI powders were performed at Ulster University's Bio-Imaging Core Facility Unit (Northern Ireland, UK) using a FEI Quanta™ 200 (FEI Company, Eindhoven, the Netherlands) scanning electron microscope (SEM). Powders were dried at 102 °C for 4 h in a moisture oven to remove moisture, coated with gold/palladium using a Polaron E5100 sputter coating unit (Quorum Technologies Ltd., Sussex, UK) and imaged as described by Bulut-Solak *et al*. (2017). All micrographs were captured using the integrated imaging software xT microscope control and a charge-coupled device camera.

Powder physical properties and key quality attributes

Interstitial air, occluded air and powder particle size were measured using traditional methodology as described in GEA Niro (2006, A11a). Particle density was measured using a gas pycnometer (Teunou *et al*. 1999). A novel method, computerised tomography (CT) scanning, was used to measure particle size, interstitial and occluded air, and the data were compared with that obtained using the traditional approach. For CT scanning analysis, powder samples were transferred to plastic cylindrical containers mounted on a glass rod and stabilised for 1 h at 22 °C. The sample was then mounted on the sample stage in the X-ray microtomography chamber, and images were obtained using a GE Vtomex L300 CT scanner (Baker Hughes Company, Houston, Texas, USA). The X-rays were emitted at a voltage of 70 kV and a current of 220 μA from a tungsten target on a diamond window with an exposure time of 500 ms. The sample was rotated 360° and during this time 1500 radiographs were recorded and transferred to a computer for reconstruction. The sample was placed 6.5 mm from the 180 kV transmission tube, while the detector was located 800 mm from the tube, which resulted in a 120× magnification of the sample and the resolution of the scan was between 1.63 and 1.69 μm. The differentiation of powder particle and air was completed using ambient occlusion algorithms. Ambient occlusion is a model that uses a fixed number of rays with a predefined length from each background voxel (values in a normal 3D grid), and this produces a binary scalar field in all directions and counts the number of rays touching the foreground, while also computing the intersection points of the rays with the foreground (Baum and Titschack 2016; Titschack *et al*. 2018). Powder flow function, bulk density, wall friction and compressibility index were measured using a Brookfield powder flow tester (Brookfield Engineering Laboratories, Inc., Middleboro, MA, USA) using the 5-inch cell in accordance with the methodology of Crowley *et al*. (2014).

Statistical data analysis

All experimental analyses were conducted in triplicate. CT particle size distributions were calculated for each dimension from a summation of their respective size classes and categorised into 10-μm fractions. Where applicable, the data generated were subjected to one-way ANOVA. Tukey's honest significant difference post hoc test was used to determine statistically significant differences ($P < 0.05$) between mean values for different samples. Mean values were determined to have significant differences from one another at a 95% confidence level. Results are expressed as mean ± standard deviation from triplicate analysis, and statistically significant differences are identified using superscript letters.

RESULTS AND DISCUSSION

Protein denaturation, aggregation and viscosity development during thermal treatment

The protein denaturation of the unheated WPI powder (WPI_{UH}), heated (WPI_H) and heated with calcium (WPI_{HCa}), including the levels of total denatured protein, α-lactalbumin and β-lg content relative to the control (WPI_C), is shown in Table 1. The total denatured protein levels were 3.2, 64.4 and 74.4% for WPI_{UH}, WPI_H and WPI_{HCa}, respectively. These values are in agreement to those reported in the work of Joyce *et al*. (2017) who observed increasing whey protein denaturation as temperature increased in whey-dominant infant formula systems. Viscosity is known to increase with increasing severity of heat treatment and added calcium due to denaturation and aggregation (Wijayanti *et al*. 2014). All samples heated at 80 °C (Figure 1a,e,f) had comparable final viscosity regardless of calcium and protein concentrations and thermal processing hold time. Samples heated at 85 °C (Figure 1b) had significantly higher ($P < 0.05$) final viscosity compared with samples heated at 80 °C (Figure 1a). For samples heated at 90 °C (Figure 1c,d), final viscosity increased with increasing calcium concentration and hold time. Moreover, it was found that samples with final viscosity >100 mPa.s gelled within 24 h of thermal treatment (data not shown), which coincides with previous findings of Joyce *et al*. (2018) and Phan-Xuan *et al*. (2014), who investigated viscosity and denaturation of thermally processed WPI and β-lg solutions with added calcium, respectively. The particle size distribution profiles of the whey protein solutions were generally monomodal, with mean particle size increasing from 65 to 205 nm, in general accordance with increasing severity of heat treatment (Figure 2). All WPI solutions heated at 80 °C (Figure 2a,e,f) had comparable particle size distributions at different calcium concentrations, with the exception of samples containing 2.5 mM calcium (8% protein, 80 °C, 30 s; Figure 2e). In contrast, WPI solutions heated at 85 (Figure 2b) and 90 °C (Figure 2c,d) had significantly higher ($P < 0.05$) mean particle size, with the extent of these increases being greater at higher calcium addition levels. In addition, it was found that the particle size of solutions generally did not change significantly after drying (D_{50}: WPI_C 7 nm, WPI_{UH} 7 nm, WPI_H 114 nm and WPI_{HCa} 132 nm). Furthermore, heat, calcium addition, protein concentration and hold time clearly affected whey protein denaturation and aggregation.

A treatment that had (a) a significant amount of colloidal aggregates, (b) did not undergo excessive aggregation post-heat treatment and (c) had a particle size distribution of 130-170 nm was the criterion set for choosing a treatment to advance to pilot-scale. Based on these requirements, a treatment of 10% protein, 90 °C, 30 s peak hold time, with 2.5 mM added calcium was taken forward for further analysis.

Colour

The treated powders had higher L^* values, and there were no significant differences ($P < 0.05$) between the treated powders, while all powders had similar values for a^* and b^* (Table 2). The ΔE values between WPI_{UH}, WPI_H and WPI_{HCa} were all <1, whereas when comparing WPI_C to WPI_{UH}, WPI_H and $WPI_{HCa,}$ they were 4.09, 4.18 and 3.58, respectively. In spite of these measured differences in colour chromaticity coordinates between samples, the powder samples were not visibly different (data not shown). The values measured and the powder appearance in this study coincide with those reported in the work of Barone *et al*. (2019) who studied high-protein content WPC and WPI powders. The results reported in this study demonstrate that while there were heat- and mineral-induced differences in denaturation and aggregation of whey proteins in solution, these differences were not evident in the colour of resultant powders.

Microstructure

The overall surface morphology of the WPI powders was analysed using scanning electron microscopy (SEM), and at a magnification of 800× (Figure 3), all samples appeared to have a heterogeneous mix of discrete small, medium and large particles. At higher magnification (1600 and 3000×), SEM analysis showed that WPI_C had a large amount of fine particulate material attached to the surface of the particles, while the surfaces of particles in WPI_{UH}, WPI_H and WPI_{HCa}

Table 1 Denatured protein content of whey protein isolate powders (WPI), control (WPI_C), unheated (WPI_{UH}), heated (WPI_H) and heated with calcium (WPI_{HCa}).

Denaturation (%)	WPI_C	WPI_{UH}	WPI_H	WPI_{HCa}
Whey protein	n/a	3.20 ± 0.20^a	64.4 ± 1.40^b	74.4 ± 3.10^c
α-Lactalbumin	n/a	2.20 ± 0.20^a	44.5 ± 3.10^b	54.8 ± 4.00^c
β-Lactoglobulin	n/a	3.60 ± 0.20^a	70.8 ± 0.40^b	80.7 ± 2.50^c

n/a = not applicable.

[abc]Different superscript letters, within a row, indicate statistically significant differences ($P < 0.05$).

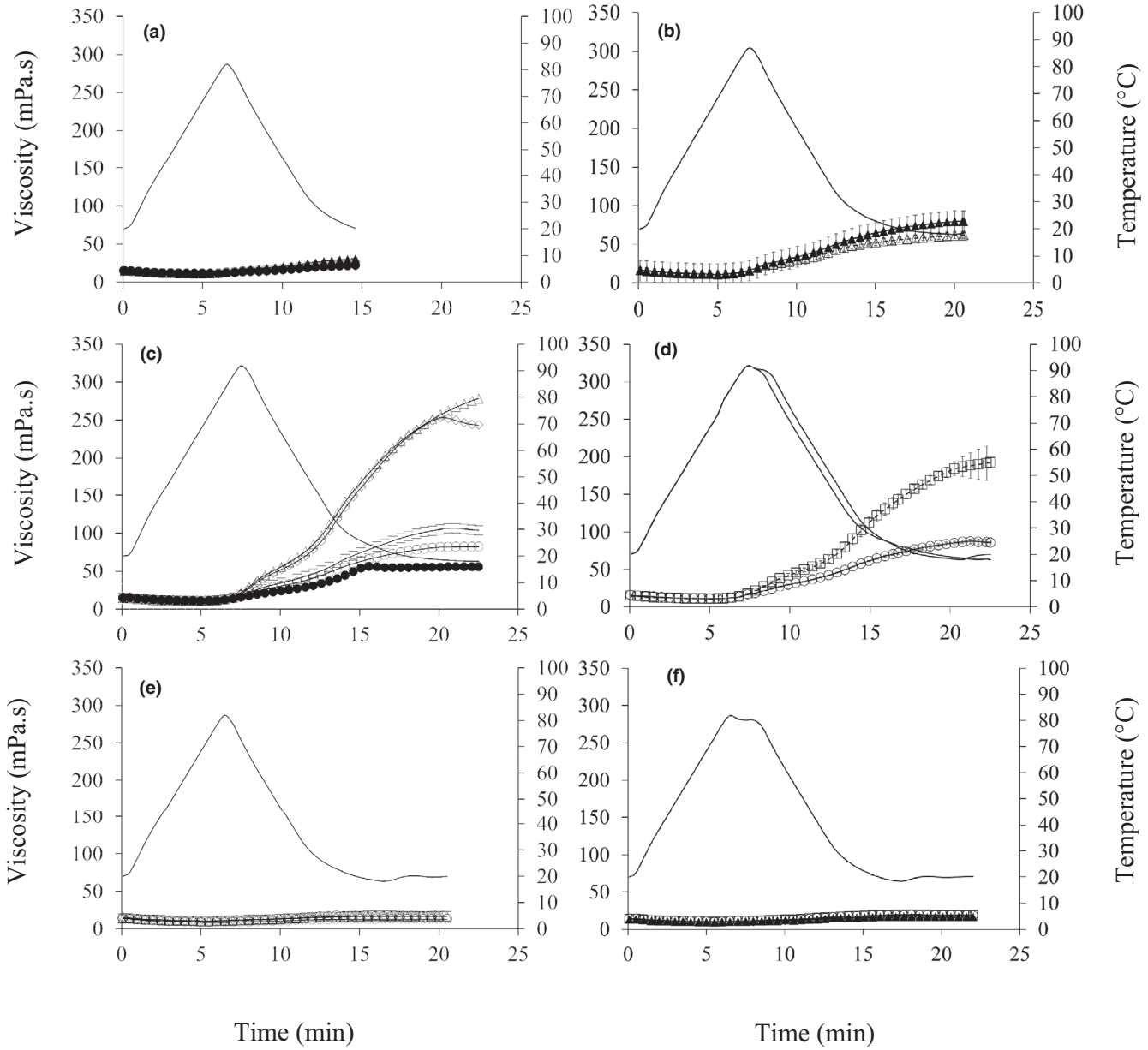

Figure 1 Temperature (solid lines) and viscosity (symbols) of whey protein isolate (WPI_C) solutions (protein, *w/v*) during laboratory-scale trials processed under different conditions for protein content, peak temperature and holding time, respectively: (a) 10%, 80 °C, 30 s; (b) 10%, 85 °C, 30 s; (c) 10%, 90 °C, 30 s; (d) 10%, 90 °C, 60 s; (e) 8%, 80 °C, 30 s and (f) 8%, 80 °C, 120 s with varying amounts of calcium: 0.0 mM (●), 2.5 mM (○), 3.0 mM (□), 3.5 mM (◇), 4.0 mM (Δ), 4.5 mM (▲).

did not display any evidence of such particulates (Figure 3). In general, powder particles in all samples displayed spherical-type morphology, with holes evident in individual powder particles, which is in agreement with the findings of Barone *et al*. (2019) who investigated the microstructure of agglomerated WPC 80 powder. Compared with WPI_C, the powder particles in samples WPI_{UH}, WPI_H and WPI_{HCa} appeared more hollow, with protrusions and holes. WPI_{HCa} and WPI_H also displayed some evidence of cohesion between powder particles. In the work of Kim *et al*. (2005b), the authors showed that denatured β-lg in solution had increased viscoelastic properties due to a decrease in α-helix content and increased flexibility of the protein molecule, which allowed for enhanced powder particle integrity, thereby limiting hole formation during spray-drying. The current study demonstrates that denaturation and aggregation of whey proteins altered particle size and morphology of spray-dried WPI powders.

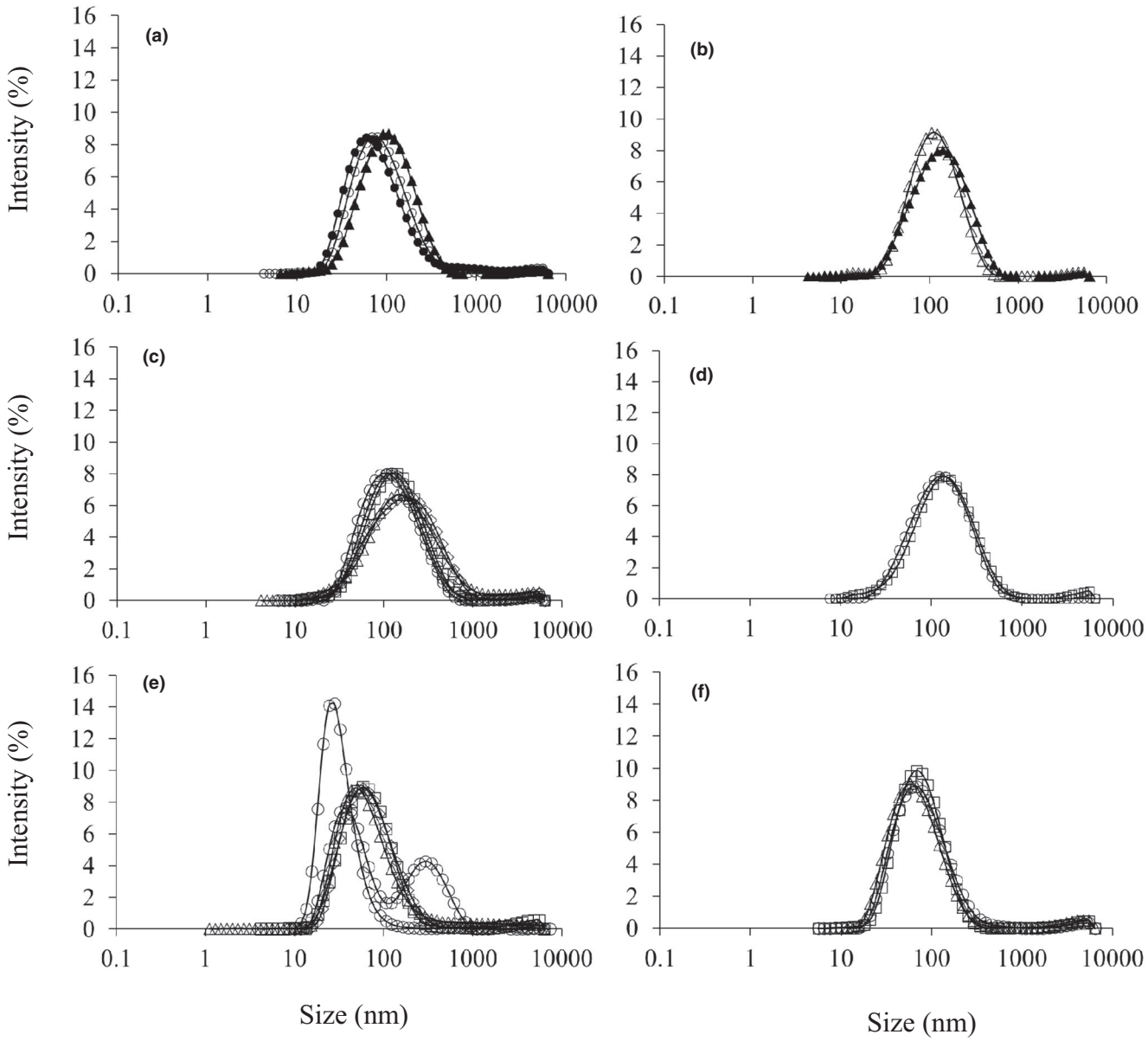

Figure 2 Particle size of whey protein isolate (WPI_C) solutions processed under different conditions for protein content, peak temperature and holding time, respectively: (a) 10%, 80 °C, 30 s; (b) 10%, 85 °C, 30 s; (c) 10%, 90 °C, 30 s; (d) 10%, 90 °C, 60 s; (e) 8%, 80 °C, 30 s; and (f) 8%, 80 °C, 120 s with varying amounts of calcium: 0.0 mM (●), 2.5 mM (○), 3.0 mM (□), 3.5 mM (◇), 4.0 mM (Δ), 4.5 mM (▲).

Powder physical properties

Computerised tomography (CT) scan analysis (Figure 4) showed that the proportion of powder particles with diameter ≤30 μm was 52.6, 84.0, 74.5 and 41.9% for WPI_C, WPI_{UH}, WPI_H and WPI_{HCa}, respectively. This indicates that heat-induced aggregation and denaturation prior to spray-drying influenced powder particle size distribution. The larger particle size of WPI_C compared with WPI_H and WPI_{HCa} is likely from the high total solid content used in its manufacturing. Moreover, the hollow particles visualised using SEM are a direct result of the rotary atomiser used in this experiment, which increased the incorporation of air into the droplets due to air aspiration by the rotating wheel (O'Sullivan *et al*. 2019). These results are in agreement with previous studies which measured the particle size of WPI powders (Caillard *et al*. 2012). The particle density, occluded and interstitial air contents of the WPI powders are shown in Table 2. The particle density of WPI_{UH}, WPI_H and WPI_{HCa} was comparable, while WPI_C had a significantly higher ($P < 0.05$) particle density, and overall, these results are higher than values (1.06 ± 0.01 g/cm^3) reported in previous studies (Ji *et al*. 2017). The use of the

Table 2 Occluded and interstitial air, particle density, compressibility index and colour of whey protein isolate (WPI) powders, control (WPI_C), unheated (WPI_{UH}), heated (WPI_H) and heated with calcium (WPI_{HCa}).

Powder properties	Units	Method	WPI_C	WPI_{UH}	WPI_H	WPI_{HCa}
Particle density	g/cm^3	GP	1.17 ± 0.00^a	1.12 ± 0.09^b	1.13 ± 0.01^b	1.12 ± 0.01^b
Occluded air	%	CT	3.8 ± 0.4^a	2.3 ± 0.2^b	3.8 ± 0.3^a	3.9 ± 0.2^a
Occluded air	%	T	2.0^b	2.7^a	2.6^a	2.5^a
Interstitial air	%	CT	36.5 ± 0.7^a	16.3 ± 0.2^c	24.5 ± 0.9^b	35.7 ± 1.1^a
Interstitial air	%	T	22.7^d	62.5^a	50.0^b	46.7^c
Compression index	n/a	PFT	41.0 ± 2.5^a	41.4 ± 0.5^a	42.8 ± 2.5^a	47.3 ± 5.4^a
Colour parameters						
*L**	n/a	C	69.4 ± 0.31^b	74.8 ± 0.60^a	74.9 ± 0.57^a	74.1 ± 0.03^a
*a**	n/a	C	-0.97 ± 0.01^a	-0.84 ± 0.03^a	-0.73 ± 0.05^a	-1.18 ± 0.02^a
*b**	n/a	C	5.67 ± 0.02^a	5.17 ± 0.02^a	5.08 ± 0.01^a	5.35 ± 0.01^a

T = traditional method, CT = computerised tomography, GP = gas pycnometry, PFT = powder flow tester, C = colorimeter, n/a = not applicable, ° = degrees.

[abc]Different superscript letters, within a row, indicate statistically significant differences ($P < 0.05$).

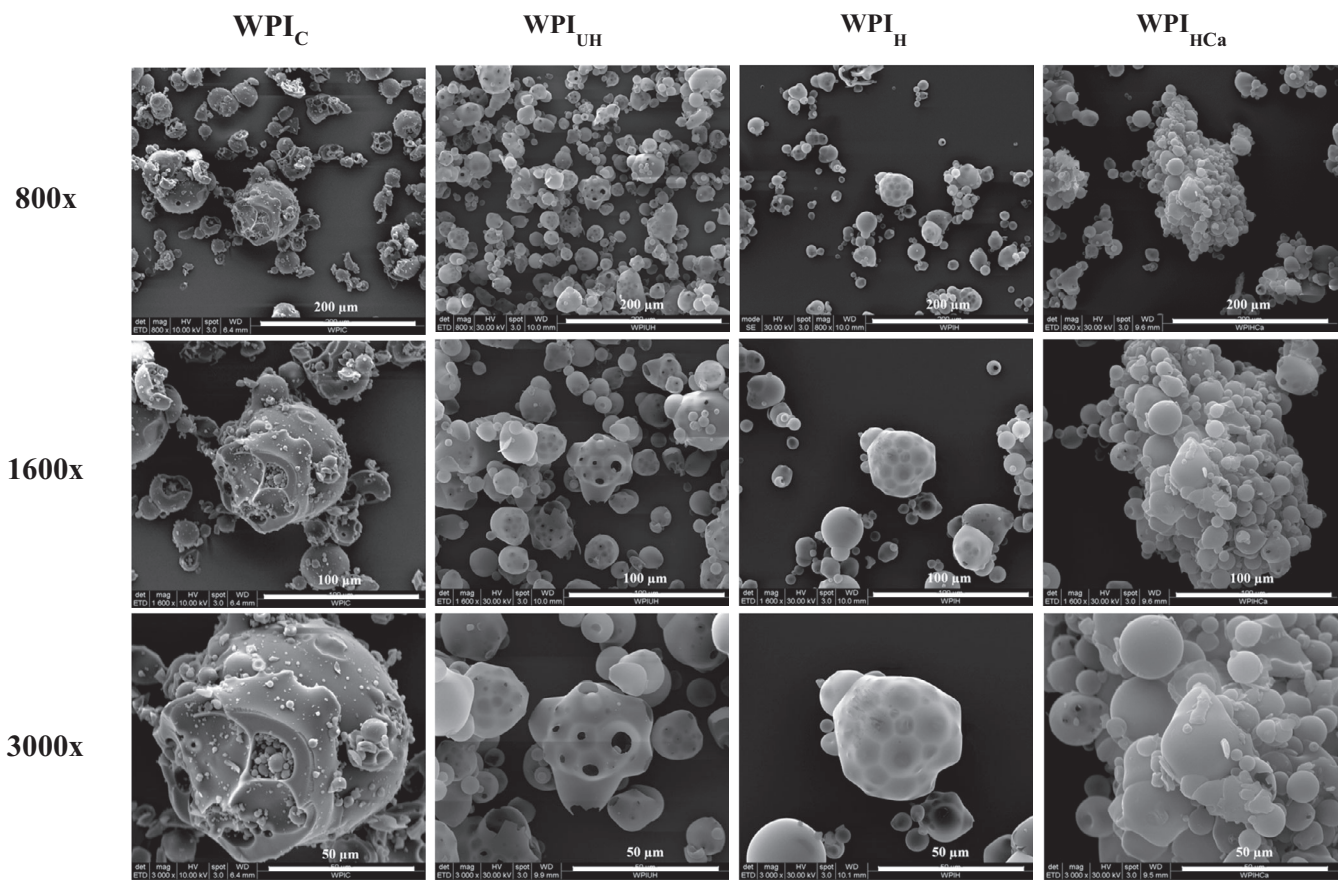

Figure 3 Scanning electron micrographs of whey protein isolate control powder (WPI_C), unheated (WPI_{UH}), heated to 90 °C for 30 s (WPI_H) and heated to 90 °C for 30 s with 2.5 mM calcium addition (WPI_{HCa}) at 3 different magnifications (800, 1600 and 3000×).

traditional GEA methodology (T) revealed that the volume of occluded air in WPI_{UH}, WPI_H and WPI_{HCa} was similar, while the level was significantly lower ($P < 0.05$) in WPI_C. The lower particle density and higher volume of occluded air in resultant WPI powders were caused by the use of a rotary atomiser which increased the incorporation of air into

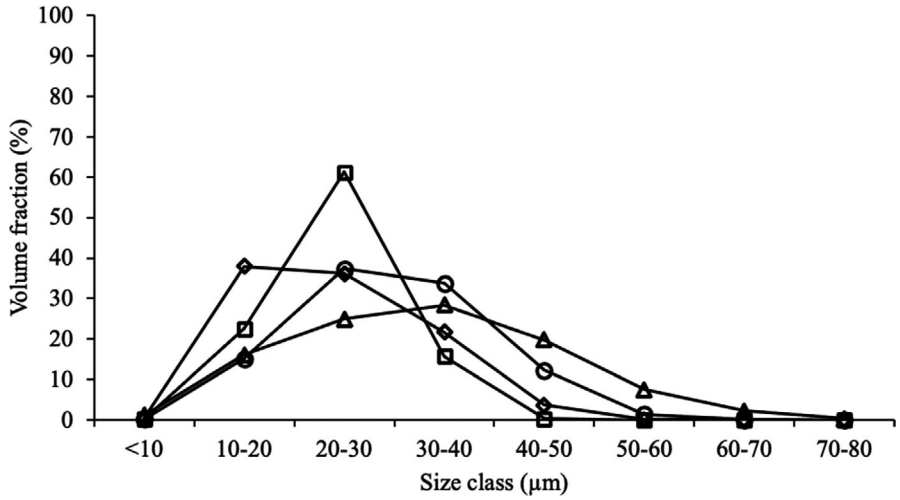

Figure 4 Powder particle size distributions using computerised tomography (CT) scanning of the control powder (WPI_C; ○), unheated (WPI_{UH}; □), heated (WPI_H; ◇) and heated with 2.5 mM calcium addition (WPI_{HCa}; Δ).

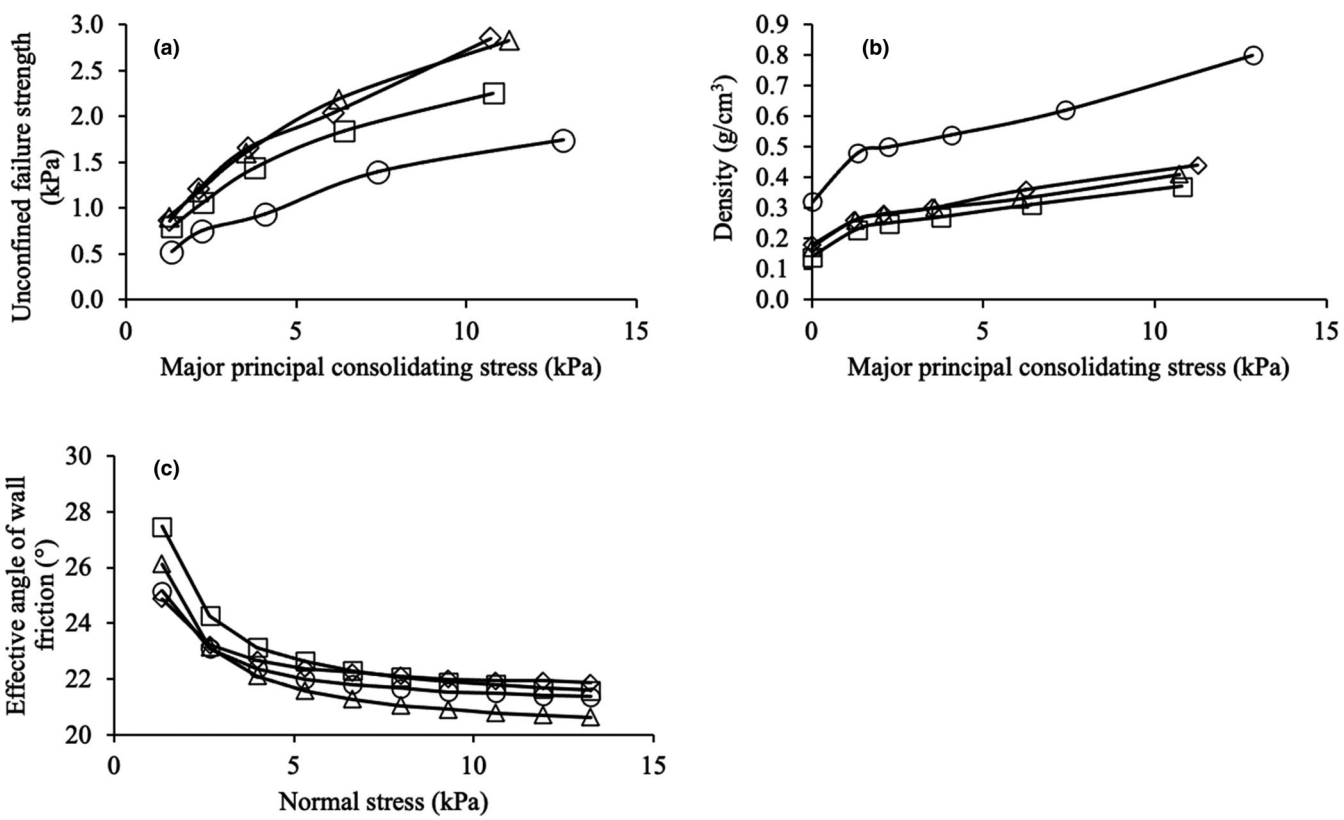

Figure 5 Flow function (a), bulk density (b) and wall friction (c) of a control whey protein isolate powder (WPI_C; ○) and unheated (WPI_{UH}; □), heated (WPI_H; ◇) and heated with 2.5 mM calcium addition (WPI_{HCa}; Δ).

the droplets due to air aspiration, thereby decreasing particle density (O'Sullivan *et al*. 2019). Furthermore, the CT scanning approach showed that the volumes of occluded air in WPI_C, WPI_H and WPI_{HCa} were similar, while WPI_{UH} had significantly lower ($P < 0.05$) volumes of occluded air. The volumes of interstitial air, as measured using the CT scanning approach, increased with powder particle size ($WPI_{UH} < WPI_H < WPI_{HCa}$), while the volume of interstitial air measured using the traditional approach did not follow a corresponding trend ($WPI_{HCa} < WPI_H < WPI_{UH}$).

These differences in measured values of occluded and interstitial air may be attributed to the fact that CT scanning utilises high-quality 3D images from 2D slices to differentiate air volumes, whereas the traditional methodology uses density to calculate air volumes. The data generated for occluded and interstitial air utilising the traditional methodology agreed with the results reported by Sadek *et al*. (2014). It is evident that further investigation is needed on the application of CT scanning to differentiate and measure occluded and interstitial air in dairy powders. Furthermore, CT scanning can be used to determine the physical properties through high-quality images. This is beneficial when analysing dairy powders, which can vary in size and microstructure based on formulation, unit operation and processing parameters used.

Powder bulk handling properties

Flow function, bulk density and wall friction properties of WPI powders are shown in Figure 5. At low uniaxial force, all samples were easy flowing as indicated by the inverse slope of the flow function ($4 <$ flow factor (FF) < 10), whereas, when the force applied was increased, WPI_H and WPI_{HCa} became cohesive ($2 < FF < 4$), and WPI_C and WPI_{UH} remained easy flowing ($4 < FF < 10$). This indicates that denaturation and aggregation of whey protein increased cohesiveness of WPI powders. The findings of this study are in agreement to those from the work of Schmidmeier *et al*. (2019) and Barone *et al*. (2019) which reported the flowability of agglomerated whey protein concentrate powders, with powders in the latter study having altered protein profiles. In addition, the bulk density of WPI_{UH}, WPI_H and WPI_{HCa} was similar. Furthermore, the angle of wall friction and the compressibility index were comparable for all samples (Table 2), with values for bulk density, angle of wall friction and compressibility being in agreement with results from previous studies (Schuck *et al*. 2012). In general, characteristics that influence flow properties of powders include particle size (Figure 4) and shape (Figure 3), bulk and particle density (Table 2), surface structure (Figure 3) and composition, moisture and fat content (Kim *et al*. 2005a; Schuck *et al*. 2012). The results of the present study clearly show that controlled whey protein denaturation and aggregation altered powder particle surface structures, thereby increasing interparticle interactions and decreasing the flowability of WPI powders.

CONCLUSIONS

In this study, whey protein particle size was modulated by heat- and mineral-induced aggregation followed by spray-drying to investigate the effects of such changes on structural, physical and bulk handling properties of the resultant powders. Increasing the levels of whey protein denaturation and aggregation before spray-drying resulted in larger, less dense, more porous powder particles, with bubble-like microstructures and increased cohesiveness during powder flow than powders with higher levels of native whey protein. The use of novel CT scanning methodology was compared to more traditional approaches for measuring particle size, powder structural and physical properties, and while promising, additional research is needed to fully realise the potential of this technique.

ACKNOWLEDGEMENT

This work was supported by the Food Institutional Research Measure (FIRM) project 'Developing the next generation of high protein spray-dried dairy powders with enhanced hydration properties' (DAIRYDRY 15-F-679) funded by both the Irish Department of Agriculture, Food and the Marine and the Department of Agriculture, Environment and Rural Affairs in Northern Ireland. The authors would like to acknowledge and thank David Waldron for powder pictures and Agnieszka Furman from Waterford Institute of Technology (Waterford, Ireland) for sample preparation and CT scanning.

AUTHOR CONTRIBUTIONS

Jacob R Guralnick: Conceptualization; data curation; formal analysis; methodology; writing-original draft; writing-review & editing. **Ram R Panthi**: Conceptualization; methodology; formal analysis; supervision; writing-review & editing. **Francesca Bot**: Methodology; supervision; writing-original draft; writing-review & editing. **Valeria L Cenini**: Formal analysis; investigation; writing-original draft; writing-review & editing. **Barry MG O'Hagan**: Formal analysis; resources; supervision; writing-review & editing. **Shane V Crowley**: Conceptualization; supervision; writing-review & editing. **James A O'Mahony**: Conceptualization; funding; resources; supervision; writing-review & editing.

DATA AVAILABILITY STATEMENT

The data that support the findings of this study are available from the corresponding author upon reasonable request.

REFERENCES

Akkermans C, Van der Goot A J, Venema P, Van der Linden E and Boom R M (2008) Properties of protein fibrils in whey protein isolate solutions: Microstructure, flow behaviour and gelation. *International Dairy Journal* **18** 1034–1042.

Amagliani L, O'Regan J, Kelly A L and O'Mahony J A (2016) Physical and flow properties of rice protein powders. *Journal of Food Engineering* **190** 1–9.

Anandharamakrishnan C, Rielly C D and Stapley A G F (2007) Effects of process variables on the denaturation of whey proteins during spray drying. *Drying Technology* **25** 799–807.

Barone G, O'Regan J and O'Mahony J A (2019) Influence of composition and microstructure on bulk handling and rehydration properties

of whey protein concentrate powder ingredients enriched in α-lactalbumin. *Journal of Food Engineering* **255** 41–49.

Baum D and Titschack J. (2016) Cavity and pore segmentation in 3D images with ambient occlusion. In *EuroVis*, pp 1–12. Groningen, the Netherlands: Zuse Institute Berlin.

Both E M, Nuzzo M, Millqvist-Fureby A, Boom R M and Schutyser M A I (2018) Morphology development during single droplet drying of mixed component formulations and milk. *Food Research International* **109** 448–454.

Bouaouina H, Desrumaux A, Loisel C and Legrand J (2006) Functional properties of whey proteins as affected by dynamic high-pressure treatment. *International Dairy Journal* **16** 275–284.

Buggy A K, McManus J J, Brodkorb A, Hogan S A and Fenelon M A (2018) Pilot-scale formation of whey protein aggregates determine the stability of heat-treated whey protein solutions—Effect of pH and protein concentration. *Journal of Dairy Science* **101** 10819–10830.

Bulut-Solak B, Alonso-Miravalles L and O'Mahony J A (2017) Composition, morphology and pasting properties of *Orchis anatolica* tuber gum. *Food Hydrocolloids* **69** 483–490.

Caillard R, Guillet-Nicolas R, Kleitz F and Subirade M (2012) Tabletability of whey protein isolates. *International Dairy Journal* **27** 92–98.

Çakir-Fuller E (2015) Enhanced heat stability of high protein emulsion systems provided by microparticulated whey proteins. *Food Hydrocolloids* **47** 41–50.

Crowley S V, Gazi I, Kelly A L, Huppertz T and O'Mahony J A (2014) Influence of protein concentration on the physical characteristics and flow properties of milk protein concentrate powders. *Journal of Food Engineering* **135** 31–38.

Foegeding E A, Davis J P, Doucet D and McGuffey M K (2002) Advances in modifying and understanding whey protein functionality. *Trends in Food Science & Technology* **13** 151–159.

Gaiani C, Morand M, Sanchez C, Tehrany E A, Jacquot M, Schuck P, Jeantet R and Scher J (2010) How surface composition of high milk proteins powders is influenced by spray-drying temperature. *Colloids and Surfaces B: Biointerfaces* **75** 377–384.

Gaucheron F (2010) Analysing and improving the mineral content of milk. In *Improving the Safety and Quality of Milk*, 1st edn, pp 207–228. Griffiths, M, eds. Cambridge, UK: Woodhead Publishing Limited.

GEA Niro (2006) A11a – Powder bulk density, occluded air and interstitial air by pycnometer. [Internet document] URL https://www.gea.com/en/binaries/A%2011%20a%20-%20Particle%20Density%2C%20Occluded%20Air%20and%20Interstitial%20Air%20by%20Air%20Pycnometer_tcm11-30919.pdf.

Hogan S A and O'Callaghan D J (2013) Moisture sorption and stickiness behaviour of hydrolysed whey protein/lactose powders. *Dairy Science & Technology* **93** 505–521.

Huppertz T, Fox P F and Kelly A L (2004) High pressure-induced denaturation of α-lactalbumin and β-lactoglobulin in bovine milk and whey: a possible mechanism. *Journal of Dairy Research* **71** 489–495.

IDF (2004) International IDF standard 20A. In *Dried Milk – Determination of Moisture Content*. Brussels, Belgium: International Dairy Federation.

IDF (2014) International IDF standard 20A. In *Milk and Milk Products – Determination of Nitrogen Content - Part 1: Kjeldahl Principle and Crude Protein Calculation*. Brussels, Belgium: International Dairy Federation.

Ji J, Cronin K, Fitzpatrick J and Miao S (2017) Enhanced wetting behaviours of whey protein isolate powder: The different effects of lecithin addition by fluidised bed agglomeration and coating processes. *Food Hydrocolloids* **71** 94–101.

Joyce A M, Brodkorb A, Kelly A L and O'Mahony J A (2017) Separation of the effects of denaturation and aggregation on whey-casein protein interactions during the manufacture of a model infant formula. *Dairy Science and Technology* **96** 787–806.

Joyce A M, Kelly A L and O'Mahony J A (2018) Controlling denaturation and aggregation of whey proteins during thermal processing by modifying temperature and calcium concentration. *International Journal of Dairy Technology* **71** 446–453.

Kim D A, Cornec M and Narsimhan G (2005b) Effect of thermal treatment on interfacial properties of β-lactoglobulin. *Journal of Colloid and Interface Science* **285** 100–109.

Kim E H -J, Chen X D and Pearce D (2005a) Effect of surface composition on the flowability of industrial spray-dried dairy powders. *Colloids and Surfaces B: Biointerfaces* **46** 182–187.

Lagrange V, Whitsett D and Burris C (2015) Global market for dairy proteins. *Journal of Food Science* **80** A16–A22.

Meza B E, De Piante V D A, Marino F, Sihufe G A, Peralta J M and Zorrilla S E (2019) Characterisation of soluble aggregates from commercial whey protein concentrate suspensions: Effect of protein concentration, pH, and heat treatment conditions. *International Journal of Dairy Technology* **73** 429–436.

Nuzzo M, Sloth Overgaard J, Bergenståhl B and Millqvist-Fureby A (2017) The morphology and internal composition of dried particles from whole milk—From single droplet to full scale drying. *Food Structure* **13** 35–44.

O'Sullivan J J, Norwood E A, O'Mahony J A and Kelly A L (2019) Atomisation technologies used in spray drying in the dairy industry: A review. *Journal of Food Engineering* **243** 57–69.

Ooi J Y (2015) *Whey protein denaturation and aggregation during high temperature-short time thermal processing as influenced by temperature and ionic strength*. MSc Degree. University College Cork.

Phan-Xuan T, Durand D, Nicolai T, Donato L, Schmitt C and Bovetto L (2014) Heat induced formation of beta-lactoglobulin microgels driven by addition of calcium ions. *Food Hydrocolloids* **34** 227–235.

Ryan K N, Vardhanabhuti B, Jaramillo D P, van Zanten J H, Coupland J N and Foegeding E A (2012) Stability and mechanism of whey protein soluble aggregates thermally treated with salts. *Food Hydrocolloids* **27** 411–420.

Sadek C, Li H, Schuck P, Fallourd Y, Pradeau N, Le Floch-Fouéré C and Jeanet R (2014) To what extent do whey and casein micelle proteins influence the morphology and properties of the resulting power? *Drying Technology* **32** 1540–1551.

Schmidmeier C, O'Gorman C, Drapala K P, Waldron D S and O'Mahony J A (2019) Elucidation of factors responsible for formation of white flecks in reconstituted fat filled milk powders. *Colloids and Surfaces A: Physicochemical and Engineering Aspects* **575** 245–255.

Schuck P, Dolivet A and Jeantet R (2012) Determination of flowability and floodability indices. In *Analytical Methods for Food and Dairy Powders*, 1st edn, pp 129–143. Hoboken, NJ: Wiley-Blackwell.

Schuck P, Mejean S, Dolivet A, Gaiani C, Banon S, Scher J and Jeantet R (2007) Water transfer during rehydration of micellar casein powders. *Le Lait* **87** 424–432.

Sinha R, Radha C, Prakash J and Kaul P (2007) Whey protein hydrolysate: Functional properties, nutritional quality and utilization in beverage formulation. *Food Chemistry* **101** 1484–1491.

Teunou E, Fitzpatrick J and Synnott E (1999) Characterisation of food powder flowability. *Journal of Food Engineering* **39** 31–37.

Titschack J, Baum D, Matsuyama K, Boos K, Färber C, Kahl W -A, Ehrig K, Meinel D, Soriano C and Stock S R (2018) Ambient occlusion – A powerful algorithm to segment shell and skeletal intrapores in computed tomography data. *Computers & Geosciences* **115** 75–87.

Wijayanti H B, Bansal N and Deeth H C (2014) Stability of whey proteins during thermal processing: A review. *Comprehensive Reviews in Food Science and Food Safety* **13** 1235–1251.

